



Citation for published version:

Noble, JPP, Bending, SJ, Muxworthy, AR & Hill, AK 2023, 'A simplified model for minor and major loop magnetic hysteresis and its application for inference of temperature in induction heated particle beds', *Journal of Physics D: Applied Physics*, vol. 56, no. 49, 495003. <https://doi.org/10.1088/1361-6463/acf13f>

DOI:

[10.1088/1361-6463/acf13f](https://doi.org/10.1088/1361-6463/acf13f)

Publication date:

2023

Document Version

Publisher's PDF, also known as Version of record

[Link to publication](#)

Publisher Rights

CC BY

University of Bath

Alternative formats

If you require this document in an alternative format, please contact:
openaccess@bath.ac.uk

General rights

Copyright and moral rights for the publications made accessible in the public portal are retained by the authors and/or other copyright owners and it is a condition of accessing publications that users recognise and abide by the legal requirements associated with these rights.

Take down policy

If you believe that this document breaches copyright please contact us providing details, and we will remove access to the work immediately and investigate your claim.

A simplified model for minor and major loop magnetic hysteresis and its application for inference of temperature in induction heated particle beds

Jonathan P P Noble^{1,*} , Simon J Bending¹ , Adrian R Muxworthy^{2,3} and Alfred K Hill^{1,*} 

¹ Centre for Sustainable and Circular Technologies, University of Bath, The Avenue, Claverton Down, Bath BA2 7AY, United Kingdom

² Department of Earth Science and Engineering, Imperial College London, South Kensington Campus, London SW7 2AZ, United Kingdom

³ Department of Earth Sciences, University College London, Gower Street, London WC1E 6BT, United Kingdom

E-mail: a.k.hill@bath.ac.uk and jon.noble.ceng@gmail.com

Received 30 May 2023, revised 10 August 2023

Accepted for publication 17 August 2023

Published 21 September 2023



CrossMark

Abstract

In this work, a LangArc model is presented that successfully fits both major and minor hysteresis loops of a bed of magnetic particles in real time using instruments that detect changes in the magnetic field strength, such as *in-situ* pick-up coils. A novel temperature measurement application is demonstrated based on a real-time characterisation of a magnetic material, in this case magnetite, as a function of temperature. Magnetic hysteresis can be used to provide useful induction heating in a packed bed of magnetic materials. This can be used for general heating and to provide energy to chemical reactions in chemical processes. Accurate temperature measurement of magnetic particles under induction heating is a well-known challenge: conventional techniques give a single-point measurement, and are subject to inaccuracy due to self-heating of the instrument tip. Thermal lag can be problematic given the rapid heating rates that are characteristic of induction heating. The LangArc inferred temperature measurement technique is shown to detect heating rates in excess of $30\text{ }^{\circ}\text{C}\cdot\text{s}^{-1}$, under which circumstances an in-bed thermocouple was shown to lag by as much as $180\text{ }^{\circ}\text{C}$. This new method has significant importance for temperature measurement in applications involving the induction heating of magnetic materials as it avoids the location of an instrument inside the magnetic particle bed and is highly responsive under rapid heating where other techniques can give misleading results.

* Authors to whom any correspondence should be addressed.



Original content from this work may be used under the terms of the [Creative Commons Attribution 4.0 licence](https://creativecommons.org/licenses/by/4.0/). Any further distribution of this work must maintain attribution to the author(s) and the title of the work, journal citation and DOI.

Supplementary material for this article is available [online](#)

Keywords: LangArc model, magnetic hysteresis, temperature measurement, induction heating, magnetic induction heating

(Some figures may appear in colour only in the online journal)

1. Introduction

The use of induction heating in providing heat for chemical conversions is attracting much research attention [1, 2]. It allows zero carbon electricity to be used in chemical reactions giving intensified chemical processes with highly controllable and rapid heating rates. In the heating of magnetic particles, it can be designed to approach uniform volumetric heating whereas other methods require high-temperature heat-transfer surfaces which can produce fouling, side-reactions or increased energy losses. It can also provide chemical process heating at temperatures well above 250 °C, which normally requires a gas-fired furnace. There are a number of specific challenges associated with taking measurements within a strong alternating magnetic field. It is difficult to minimise eddy current heating in the instrument and prevent melting of the instrument components and wires. Measuring temperature is particularly difficult, as self-heating of the temperature instrument can lead to a thermocouple tip that is hotter than the surrounding bed, and not representative of the bed temperature. Rapid bed heating is a significant advantage of induction heating but provides an additional temperature measurement challenge. A thermocouple can take several seconds to respond to rapidly changing bed temperatures due to the thermal mass and rate of heat transfer into the thermocouple (thermal lag) [3], during which time it will under- or over-report the bed temperature. This could lead to problems controlling the start-up of an induction heated reactor due to overshooting the desired temperature set-point.

This paper proposes a novel concept for inferring temperature from the shape of the magnetic hysteresis loop to overcome the thermal lag in measuring temperature in chemical process heaters and reactors. This is underpinned by a magnetic model that is sufficiently accurate to reproduce the hysteresis loop features and shape at a variety of temperatures and applied field strengths. There are a number of fundamental models of ferromagnetisation, such as the Priesach, Stoner–Wohlfarth or Jiles–Atherton models [4, 5]. These models can be accurate in reproducing the hysteresis loops but may require saturated hysteresis loop data to determine the model parameters and are difficult to practically apply due to their complexity and the magnetisation being expressed as a transcendental function of itself. It may not be possible to fully saturate a magnetic material depending on the equipment available, and Noble *et al* demonstrated that minor hysteresis loops for an induction heated sample may be measured *in-situ* using pickup coil magnetometry. A simplified model of magnetisation is required for inferring a magnetic sample temperature in real-time due to the rapid heating rates of induction heating of magnetic samples [6] and the need to use low cost, reliable digital

signal processing to replicate this technique in the industrial setting of a chemical synthesis process. There are a number of criteria that a model of magnetic hysteresis must satisfy to be practically applied to induction heating hysteresis loops. The model should approximate the magnetisation curves for both major (saturated) and minor hysteresis loops; approximate the Rayleigh law of magnetisation for small applied field strengths; converge on the saturation magnetisation for both large positive and negative applied field strengths; have a definite, monomodal derivative, approximating the material magnetic susceptibility; and have a definite integral, such that the hysteresis heating power can be directly determined across a range of temperatures and applied field strengths.

Noble *et al* [6] established a semi-theoretical arctangent model that successfully models the magnetic hysteresis heating power at applied field strengths well below saturation. This model will be referred to as the LineArc model due to the presence of both linear and arctangent terms. It relates the magnetisation, M , to the applied field strength, H , based on the LineArc model parameters y_0 , A , w and x_c , which are all functions of temperature. A loop closure variable, c_1 , is used to ensure that the minor hysteresis loop is a closed curve. It is a function of the peak applied field strength, \hat{H} . In this paper, the LineArc parameter x_c has been relabelled as H_p , and it will be shortly demonstrated that this parameter is equal to the applied field strength at the peak susceptibility of the major hysteresis loop.

$$M = y_0 H + \frac{A}{\pi} \left[\operatorname{atan} \left(\frac{2}{w} (H \mp H_p) \right) \pm c_1 \right] \quad (1)$$

$$c_1 = \frac{1}{2} \left[\operatorname{atan} \left(\frac{2}{w} (\hat{H} + H_p) \right) - \operatorname{atan} \left(\frac{2}{w} (\hat{H} - H_p) \right) \right] \quad (2)$$

Inferring temperature from magnetic hysteresis loops is complicated by the shape of the minor loop parameters as a function of temperature. The presence of a maximum means that a single value of power, remanence, coercivity or maximum magnetisation corresponds to two different temperatures (figure 1). These parameters have a flat curve near the peak, with little change in value across a wide temperature range. This making it difficult to accurately resolve the temperature from each parameter measurement. These ambiguities can be removed by using multiple features of the minor hysteresis loop to determine the temperature, as the peak in each parameter occurs at different temperatures.

This paper develops the LineArc model to better fit the minor hysteresis loop shape by revising the reversible magnetisation term and demonstrates proof-of-concept that the tuned model can predict the temperature of a magnetite sample solely from the measured hysteresis loop.

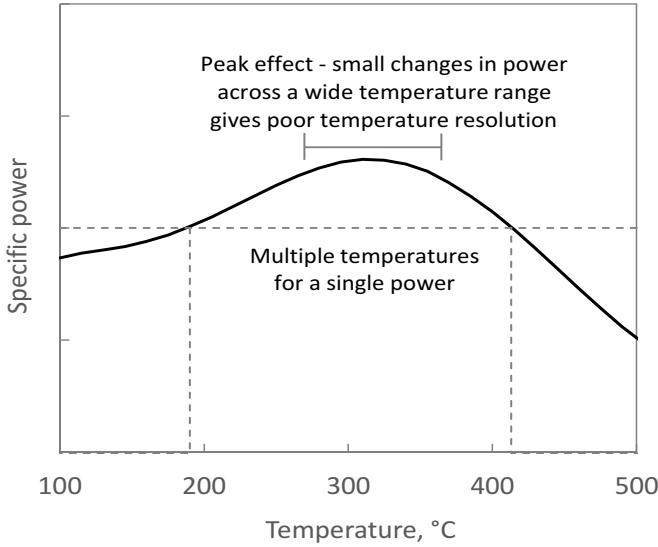


Figure 1. Schematic showing the issues with using the magnetic hysteresis power curve to determine the temperature of a magnetic sample in an alternating applied field. The hysteresis power is defined here as the integral of the hysteresis loop, equation (11). The presence of a peak means that two different temperatures are possible for a single measured power. Close to the peak, the power does not change much as a function of temperature, meaning that a small error in the power measurement could mean a 20 °C temperature measurement error.

2. Theory development

Prior to developing a revised model of hysteresis, it is useful to provide a theoretical framework for analysing the model deficiencies. This paper identifies the following novel criteria for a practically useful model of magnetic hysteresis for induction heating of chemical reactors. These criteria inform the development of a new magnetic model.

1. Approximate the magnetisation curves for both major (saturated) and minor hysteresis loops.
2. Approximate the Rayleigh law of magnetisation for small applied field strengths
3. Converge on the saturation magnetisation for both large positive and negative applied field strengths.
4. Have a definite, monomodal derivative, approximating the material magnetic susceptibility.
5. Have a definite integral, such that the hysteresis heating power can be directly determined across a range of temperatures and applied field strengths.

It is preferable to have a model that minimises the number of parameters to prevent over-fitting of the data through introduction of extra degrees of freedom. In an ideal model, these parameters would have a direct relationship with the underlying physical properties of the magnetic material, such as coercivity and remanence. This would allow the model parameters to be derived solely from the major hysteresis loop parameters as a function of temperature.

The hysteresis model can also comprise a number of functions, f_i , which represent various physical phenomena that

occur within the sample, such as a paramagnetic function and a hysteretic function. It is convenient to normalise the magnetisation of each function by dividing it by the saturation magnetisation, M_s , such that the function lies in the range from -1 to 1 . This allows the individual function terms to be combined in a weighted linear manner to give a composite equation for magnetic hysteresis (equations (3) and (4))

$$\text{Individual magnetisation functions: } \frac{M}{M_s} \Big|_i = f_i(H) \quad (3)$$

$$\text{Composite magnetisation function: } \frac{M}{M_s} = \sum \varepsilon_i \cdot f_i(H); \sum \varepsilon_i = 1 \quad (4)$$

2.1. Minor loop modelling

One approach for extending a major loop model to minor hysteresis loops is to assume that minor loops follow a similar magnetisation curve as the major loop [6]. In the instance where the applied field is smaller than that required to saturate the material, this results in forward and reverse magnetisation curves that do not close into a loop at the peak sample magnetisation. This can be resolved by introducing a loop closure constant, c . For a generic magnetisation function, this is determined by considering the reverse magnetisation curve as identical to the forward curve rotated by 180° around the origin and that the forward and reverse magnetisation curves must have the same value at the maximum magnetisation value in order for the loop to close.

$$\text{Forward magnetisation curve: } \frac{M}{M_s} = f(H) - c \quad (5)$$

$$\text{Reverse magnetisation curve: } \frac{M}{M_s} = c - f(-H) \quad (6)$$

$$\text{Loop closure: } c = \frac{1}{2} \left[f(\hat{H}) + f(-\hat{H}) \right]. \quad (7)$$

The magnetisation curve for a paramagnetic material is fully reversible and exhibits no hysteresis. In this case, the loop closure constant is zero, implying that the loop closure constant represents the degree of irreversible magnetisation. At saturation, all internal magnetic dipoles are aligned with the external applied field and must be fully reversed as the field is fully reversed and the loop closure constant becomes zero.

2.2. Low field approximation

The low-field Rayleigh law of magnetisation is a quadratic function universally applicable to magnetic materials exhibiting hysteresis [7, 8]. It is based on the susceptibility at the hysteresis loop tip, χ_r , and the Rayleigh parameter, ν . A suitable magnetic model should be equivalent to Rayleigh's law at low field strengths, which is satisfied if the function's Maclaurin series approaches a quadratic function for low applied field

strength and the higher order terms tend to zero at low field strength.

$$\text{Rayleigh law forward curve: } M = -\frac{v}{2}\hat{H}^2 + (\chi_r + v\hat{H}) \cdot H + \frac{v}{2} \cdot H^2 \quad (8)$$

$$\text{Maclaurin equivalent: } \lim_{H \rightarrow 0} M = k_0 + k_1 \cdot H + k_2 \cdot H^2 \quad (9)$$

$$k_0 = -\frac{v}{2}\hat{H}^2; k_1 = \chi_r + v\hat{H}; k_2 = \frac{v}{2}. \quad (10)$$

2.3. Definite power integral

The heating power generated through magnetic hysteresis is defined as the integral of the magnetisation curve across one cycle. This is equivalent to integrating the difference between the forward and reverse curves from $-\hat{H}$ to \hat{H} , and provides significant simplification when evaluating the integral

$$\begin{aligned} & \frac{1}{M_s} \oint M \, dH \\ &= \int_{-\hat{H}}^{\hat{H}} [f(H) + f(-H) - 2c] \cdot dH \\ &= -2\hat{H} [f(\hat{H}) + f(-\hat{H})] + \int_{-\hat{H}}^{\hat{H}} [f(H) + f(-H)] \cdot dH. \end{aligned} \quad (11)$$

2.4. Magnetisation converges on saturation magnetisation

Sigmoidal functions are ideal candidates for modelling magnetisation curves. They converge on a fixed positive and negative value at high positive and negative argument values. Takács identified a number of candidate functions for modelling major hysteresis loops [9]: the arctangent, error function, sigmoid and hyperbolic tangent (scaled logistics) functions. The authors add the Langevin, Guddermanian and polynomial sigmoid curves as additional candidate sigmoidal curves. Each of these functions satisfy the constraints of approaching saturation at high field values, having a definite derivative and power integral. This family of curves take a general form for an irreversible component of magnetisation as given in equation (12). These functions curves can also represent reversible magnetisation curves by setting H_p and c to zero. The parameter w approximates the width at half-height of the susceptibility function, dM/dH

$$\frac{M}{M_s} = f\left(\frac{2}{w}(H \mp H_p)\right) \pm c. \quad (12)$$

2.5. Developing a new hysteresis model

This paper proposes modifications to the LineArc model (equation (1)) to better reproduce the full hysteresis loop shape across all applied field strengths. The inclusion of the linear term, y_0H , is required as an arctangent-only model does not give a good data fit at low field strength. At high field strengths

the linear term predicts ever-increasing magnetisation rather than approaching the saturation magnetisation asymptotically as required for a real magnetic material. Hence it does not fully comply with the requirements for a magnetic model identified earlier in this paper, and the LineArc model cannot universally fit the hysteresis loop data across all applied field strengths.

The hysteresis loop arises from the irreversible component of magnetisation, represented by the arctangent part of the LineArc model (equation (1)). The linear term in the LineArc model represents the reversible component of magnetisation and affects hysteresis loop features such as coercivity and maximum magnetisation. It is proposed that the linear term represents a paramagnetic fraction of material in the sample. Amending the reversible magnetisation term presents an opportunity to improve the model accuracy in fitting the shape-determining features of minor hysteresis loops. An ideal model would directly relate the key features of the major hysteresis loop to the model parameters rather than relying on a parameter fit to experimental data.

The magnetisation curve for a paramagnetic material is reversible and exhibits no hysteresis. It is given by the Langevin equation, a sigmoidal curve with rotational symmetrical around the origin that is linear at low applied field strength and approaches a constant value at saturation. A new magnetic model is proposed which replaces the linear term in the LineArc model with a Langevin function to represent a reversible fraction of magnetic material (equation (13)). The arctangent function has been retained for the irreversible fraction because the LineArc model successfully approximates the hysteresis loop power (equation (14)) [6, 10]. The derivative of the Langevin function represents the susceptibility of the reversible fraction of the material. It exhibits a bell-shaped curve with a full width at half-maximum (FWHM) denoted as w_{rev} . It is distinct from the LangArc arctangent FWHM parameter, w_{irr} , which is analogous the parameter w in the original LineArc model

$$\frac{M}{M_s} \Big|_{rev} = \mathcal{L}\left(\frac{2H}{w_{rev}}\right) = \coth\left(\frac{2H}{w_{rev}}\right) - \left(\frac{w_{rev}}{2H}\right) \quad (13)$$

$$\frac{M}{M_s} \Big|_{irr} = \frac{2}{\pi} \left(\text{atan}\left(\frac{2}{w_{irr}}(H \mp H_p)\right) \pm c_2 \right). \quad (14)$$

This paper introduces a linear weighting function based on the reversible fraction, ϵ_r , in accordance equation (4) such that the total magnetisation of the sample cannot exceed the saturation magnetisation. The new model is referred to as the LangArc model (equation (15))

$$\frac{M}{M_s} = \epsilon_r \cdot \mathcal{L}\left(\frac{2H}{w_{rev}}\right) + (1 - \epsilon_r) \cdot \left(\frac{2}{\pi} \text{atan}\left(\frac{2}{w_{irr}}(H \mp H_p)\right) \pm c_2\right) \quad (15)$$

$$c_2 = \frac{1}{2} \left[\text{atan}\left(\frac{2}{w_{irr}}(\hat{H} + H_p)\right) - \text{atan}\left(\frac{2}{w_{irr}}(\hat{H} - H_p)\right) \right]. \quad (16)$$

The LangArc model is a generalised case of the LineArc model. It reduces to the LineArc model at lower field strength

as the Langevin is approximately linear for small values of argument. The equivalence of the LineArc (equation (1)) and LangArc (equation (15)) parameters are given in equations (17) and (18). The minor loop closure constants have an identical form (equations (2) and (16)), as does the hysteresis power (equation (19)), as both of these parameters are solely related to the irreversible component of magnetisation

$$y_0 \rightarrow \frac{2\varepsilon_r M_s}{3w_{\text{rev}}} \quad (17)$$

$$A \rightarrow 2(1 - \varepsilon_r) M_s \quad (18)$$

$$\frac{P_{\text{hys}}}{V} = \frac{f\mu_0(1 - \varepsilon_r)M_s}{\pi} \left[w_{\text{irr}} \cdot \ln \left(\frac{4(\hat{H} + H_p)^2 + w_{\text{irr}}^2}{4(\hat{H} - H_p)^2 + w_{\text{irr}}^2} \right) - 4H_p \left(\text{atan} \left(\frac{2(\hat{H} + H_p)}{w_{\text{irr}}} \right) + \text{atan} \left(\frac{2(\hat{H} - H_p)}{w_{\text{irr}}} \right) \right) \right] \quad (19)$$

2.6. Relating the LangArc model to the major hysteresis loop properties

The LineArc model parameters y_0 , A , w and H_p appear to be arbitrary parameters that fit the model to experimental data. The improvements made in the LangArc model provide insight in relating the model parameters to magnetic properties of the material major (saturated) hysteresis loop. At saturation, the loop closure constant c_2 is equal to zero. The applied field strength at the major loop peak susceptibility occurs when the second derivative of the magnetisation function is equal to zero. The Langevin function is approximately linear at the peak susceptibility and its second derivative approaches zero. The same is true for the linear term in the LineArc model. The second derivative of magnetisation function is the second derivative of the arctangent function only (equation (21)). The function becomes zero when the applied field strength is equal to the parameter H_p , demonstrating that H_p is the applied field strength at peak susceptibility

$$\left[\frac{d^2 \mathcal{L}(x)}{dx^2} \right]_{x=1} \approx 0 \quad (20)$$

$$\frac{d^2 M}{dH^2} = 0 \approx \frac{16(1 - \varepsilon_r)M_s}{\pi w_{\text{irr}}^3} \cdot \frac{(H - H_p)}{(4(H - H_p)^2/w_{\text{irr}}^2 + 1)^2} \quad (21)$$

Noble *et al* [6] previously asserted that the LineArc parameter A was equivalent to $2M_s$ and that H_p was approximately equal to the major loop coercivity, H_c . The new developments of the LangArc model incorporates the effects of a paramagnetic fraction on the parameter A (equation (18)) and provide a physically meaningful context for the parameter H_p to the applied field at peak susceptibility, H_p (equation (21)). The remaining LangArc model parameters can be related to the

major hysteresis loop properties by taking the linear approximations of the arctangent and Langevin functions for small arguments. This results in three equations linking the model parameters to the intrinsic major hysteresis loop parameters. The derivation is provided in the supplementary information.

$$\text{Major loop Remanence } \frac{1}{w_{\text{irr}}} \cdot (1 - \varepsilon_r) \approx \frac{\pi M_r}{4M_s H_p} \quad (22)$$

$$\text{Major loop Coercivity } \frac{1}{w_{\text{rev}}} \cdot \varepsilon_r \approx \frac{3M_r(H_p - H_c)}{2M_s H_p H_c} \quad (23)$$

$$\begin{aligned} \text{Major loop Initial susceptibility } & \frac{1}{w_{\text{irr}}} \\ & \approx \frac{1}{2H_p} \sqrt{\frac{M_r H_c}{\chi_0 H_p H_c - M_r H_p + M_r H_c} - 1}. \end{aligned} \quad (24)$$

Equations (21)–(24) demonstrate an inherent link between the LangArc model parameters and the key features of the major hysteresis loop. Such a model meets all the criteria for a practical magnetic model laid out in this paper.

The reversible term of the LangArc represents a paramagnetic fraction of material within the sample. The thermal energy associated with the particle temperature is sufficient to overcome magnetic anisotropy energy barriers in very small magnetic particles that are below the single domain threshold size. This can lead to spontaneous reversal of the magnetic field within the particle, an effect called superparamagnetism. The average time taken for the field to spontaneously reverse for a given particle size and temperature is called the Néel relaxation time [11]. Superparamagnetic particles generate excess heat when they are induction-heated at a frequency close to the relaxation time. This has a minor effect on the shape of the hysteresis when the sample has a wide particle size distribution, such as the samples used in this paper [6]. It is important that the sample magnetic characterisation is carried out at a similar frequency to that at which the temperature is to be inferred in order to minimise the frequency-based effects on the temperature inference model.

3. Results

The proof-of-concept for the temperature inference methodology is based on two samples of magnetite, Magn97-VSM and Magn97-PUC. The material in both samples was previously characterised in Noble *et al* [6]. It consists of magnetite powder with a size range of 40–200 nm, with a mean particle size of 97 nm. Sample Magn97-VSM was dispersed in epoxy cement and measured using a Princeton Measurements Vibrating Sample Magnetometer (VSM). Sample Magn97-PUC was measured as a bulk powder using pick-up coil magnetometry. The magnetic properties of the bulk powder are expected to be different to that of the same material dispersed and immobilised in the vibrating sample magnetometry due to inter-particle magnetisation effects and the ability for the bulk particles to rotate within the magnetic field. The LangArc model parameters are determined by regressing the hysteresis

loop data against a LangArc model across a range of temperatures and applied field strengths. The magnetisation measured using the VSM has an error of less than 1% and the pick-up coil magnetometry error is less than 3%. Temperature measurements using thermocouples have a maximum systematic error of 3 °C at a steady-state temperature.

3.1. Major hysteresis loop parameters

The LangArc model was found to provide an excellent fit to major hysteresis loop data for sample Magn97-VSM across a temperature range from 150 °C to 525 °C. An example fit for a temperature of 250 °C is given in figure 2. The model parameters for the major hysteresis loop data, as a function of temperature, is given in figure 3.

The saturation magnetisation at a given temperature, T , is related to the saturation magnetisation at zero Kelvin, M_{s0} , the Curie temperature, T_c , and the critical exponent, β , through the Weiss theory of ferromagnetism (equation (25)) [12, 13]

$$\frac{M_s}{M_{s0}} = \left(1 - \frac{T}{T_c}\right)^\beta. \quad (25)$$

The Curie temperature for large particle sizes of magnetite is 858 K and the critical exponent is 0.43 [13]. The temperature response of sample Magn97-VSM is described well by this relationship (figure 3(b)) and the saturation magnetisation is expected to follow the same relationship between the VSM sample and the bulk powder samples.

The model parameters fitted against the major hysteresis loops of sample Magn97-VSM show the reversible fraction, ε_r , as a continuously increasing function of temperature (figure 3(b)). The magnetite samples used in this paper have a fraction of fine particles with diameters in the tens of nanometre range. In very small particles, the thermal energy can be sufficient to allow internal magnetic dipoles to overcome internal anisotropic energy barriers within the particle leading to a reduction in their magnetic hysteresis. These particles are known as superparamagnetic and they exhibit a reversible magnetisation curve [14]. The thermal energy is proportional to the temperature, and the energy barrier is proportional to the particle volume, resulting in larger particles becoming superparamagnetic at higher temperatures [15]. This would result in an increase in the reversible fraction of material in the sample.

3.2. Determining LangArc parameters from minor hysteresis loops

Figure 3 shows that the LangArc model parameters can be directly recovered from major hysteresis loop data. This section demonstrates that this is not necessarily the case for the minor hysteresis loops due to an increase in the number of degrees of freedom at lower applied field strengths. The LangArc model is a five-parameter model and there are five key features of the hysteresis loop that constrain the model: the maximum magnetisation, \hat{M} , which is the number and strength of magnetic dipoles aligned with the magnetic field and approaches the

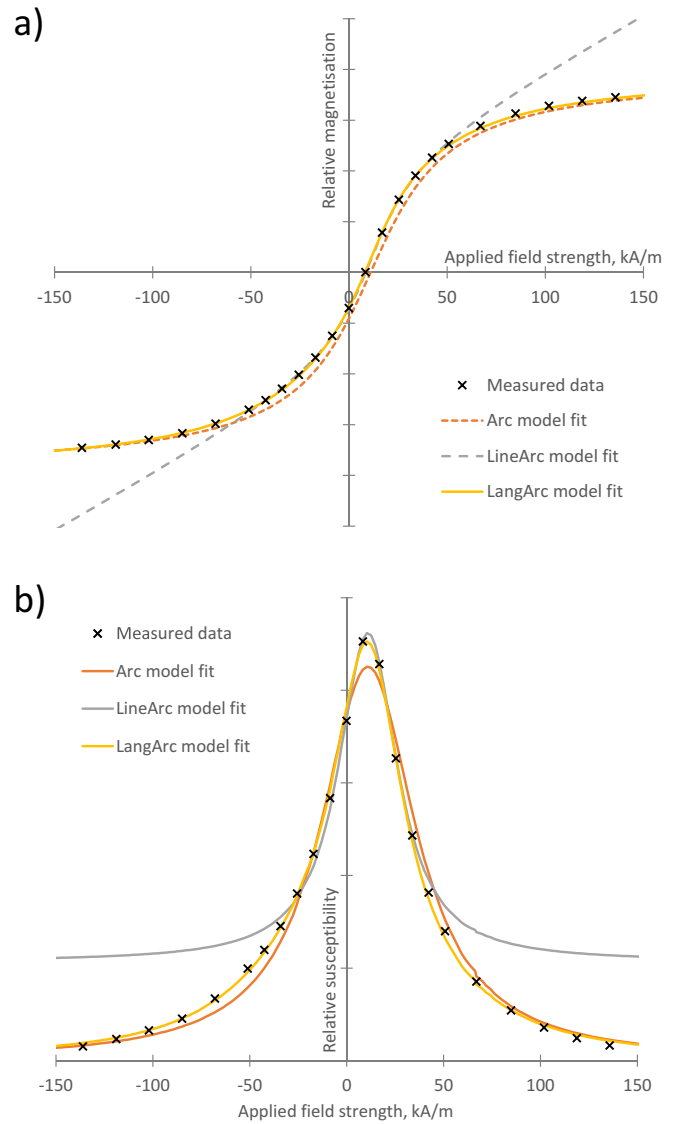


Figure 2. (a) Forward magnetisation curve for the major hysteresis loop of sample Magn97-VSM at 250 °C. Data fit to arctangent, LineArc and LangArc models. The arctangent-only model is represented by equation (14). The linear term in the LineArc model improves the data fit in the central part of the hysteresis curve but sacrifices accuracy at high field strengths. The LangArc model is an excellent fit to full major hysteresis loop. (b) Susceptibility fit for the same data. The VSM measurement gives a relative magnetisation due to a lack of information about the volume fraction of material within the sample. The model parameters can be found in figure 3.

saturation magnetisation as the applied field strength increases; the major loop magnetic remanence, M_r , which is the irreversible component of magnetisation at zero applied field; the coercivity, H_c , which represents a balanced state in which the applied field strength is such that the reversible and irreversible components of magnetisation cancel to zero magnetisation in the sample; the initial susceptibility, χ_0 , which is related to the particle shape and surface magnetic energy (conventionally indicated by the demagnetisation factor); and the total hysteresis loop power, as the integral of the hysteresis loop area. Assuming that the LangArc model represents a

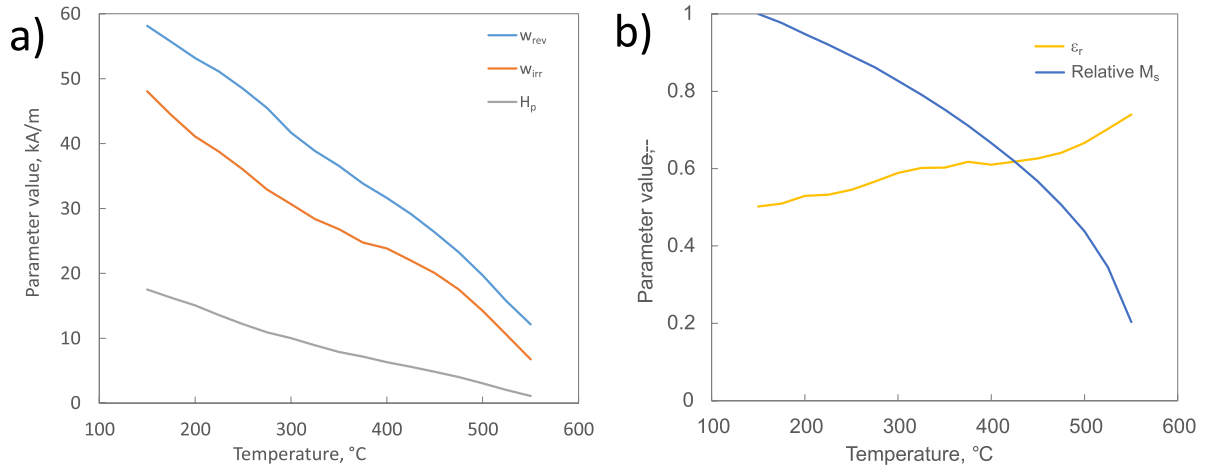


Figure 3. LangArc model parameters (equation (7)) as a function of temperature determined by regressing the major hysteresis loops of sample Magn97-VSM against the LangArc model, with the maximum magnetisation fitted against equation (25): (a) applied field strength at peak susceptibility, H_p , and reversible and irreversible width at half-height parameters, w_{rev} and w_{irr} ; (b) reversible magnetisation fraction (ϵ_r) and relative saturation magnetisation. This shows that the peak susceptibility, width at half-height and saturation magnetisation fraction all decrease with temperature, and the reversible fraction increases with temperature.

fundamental fit to both minor and major hysteresis loops, the five LangArc model parameters can be related to these five fundamental properties of the major hysteresis loop, and the model is fully constrained.

The Maclaurin series for the LangArc model is given in equation (26). The LangArc model approximates the Rayleigh law of magnetisation at low field strength (equations (8)–(10)) under the criteria that $\hat{H} < w_{rev}$, and either $\hat{H} < w_{irr}$ or $\hat{H} < H_p$

$$\frac{M}{M_s} = \left[c_2 + \frac{2(1-\epsilon_r)}{\pi} \operatorname{atan} \left(\frac{2H_p}{w_{irr}} \right) \right] + \left[\frac{2\epsilon_r}{3w_{rev}} + \frac{4(1-\epsilon_r)w_{irr}}{\pi(4H_p^2 + w_{irr}^2)} \right] H + \left[\frac{8(1-\epsilon_r)H_p w_{irr}}{\pi(4H_p^2 + w_{irr}^2)^2} \right] H^2 + o(H^3). \quad (26)$$

The Rayleigh law can be described by two parameters, χ_r and ν (equation (8)), meaning that data regressed to the LangArc model in the Rayleigh region has three degrees of freedom and the five LangArc parameters cannot be determined by data fitted to minor hysteresis loops. Additional relationships are used to mitigate this during data fitting to minor hysteresis loop data for sample Magn97-PUC. The saturation magnetisation at zero kelvin, M_{s0} , was allowed to vary during the regression, with the saturation magnetisation at the measured temperature following equation (25). During initial data fitting to the minor loop data for bulk magnetite powder, Magn97-PUC, the reversible fraction, ϵ_r , was approximately linear and equal to one at the Curie point. This linear fit relationship was arbitrarily fixed during the data regression, with the slope of the line through the Curie point allowed to vary. It is good practice to fit a model on one set of data and test the predictive power of the fit on a separate dataset, otherwise the model simply reproduces the original data. The authors fitted the model on data collected at applied field strengths

of $12.6 \text{ kA}\cdot\text{m}^{-1}$ and $18.2 \text{ kA}\cdot\text{m}^{-1}$. The determined model fit parameters are shown in figure 4.

The saturation magnetisation at zero kelvin, M_{s0} , is predicted as $287.3 \text{ kA}\cdot\text{m}^{-1}$ from the model fit to minor loop hysteresis data for Magn97-PUC. The resulting model was used to predict data collected at applied field strengths of $14.4 \text{ kA}\cdot\text{m}^{-1}$ and $16.5 \text{ kA}\cdot\text{m}^{-1}$. The raw data and model results are shown in figure 5 and standard errors associated with the model predictions are shown in table 1.

The fitted model parameters in sample Magn97-PUC follow a clear trend above $265 \text{ }^\circ\text{C}$, which is the transition away from the Rayleigh regime for an applied field of $18.2 \text{ kA}\cdot\text{m}^{-1}$ (figure 4) [6]. The shape of the curves below this temperature illustrate the difficulty in separating the five LangArc parameters in the Rayleigh region which is completely described by two parameters. Nevertheless, the constraints placed on the saturation magnetisation and reversible fraction and the regression of the remaining three parameters results in an excellent fit to the minor loop hysteresis parameters (figure 5).

3.3. Using the LangArc model to infer temperature

Having a tuned LangArc model that accurately predicts features of the hysteresis loop allows the temperature of the sample to be inferred. The temperature prediction from was performed as follows: the temperature was set as an independent variable and the model parameters were determined; the minor loop coercivity, remanence, maximum magnetisation and power were calculated from the model parameters and the required applied field strength, and these were compared to the measured values of minor loop parameters and the temperature was determined from the value which gave the minimum the sum of least squares error in the coercivity, remanence, maximum magnetisation and power. The relative error in each

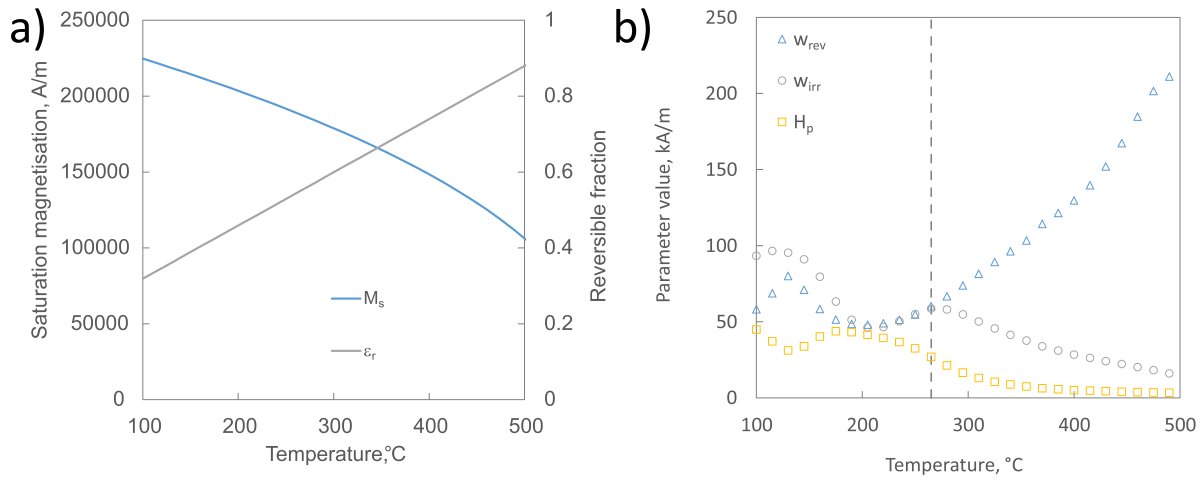


Figure 4. LangArc model fitted parameters trained against data at $12.7 \text{ kA}\cdot\text{m}^{-1}$ and $18.2 \text{ kA}\cdot\text{m}^{-1}$ for sample Magn97-PUC at a frequency of approximately 260 kHz. The vertical dashed line at $265 \text{ }^\circ\text{C}$ represents the transition from ellipsoidal hysteresis loops that can be described by Rayleigh’s law to sigmoidal loops at an applied field strength of $18.2 \text{ kA}\cdot\text{m}^{-1}$ [6]: (a) the reversible volume fraction has been fixed as a linear function passing through one at the Curie temperature, $585 \text{ }^\circ\text{C}$ for magnetite and the saturation magnetisation as a function of temperature has been fitted to equation (25). Resulting in a predicted saturation magnetisation at 0 K of $287.3 \text{ kA}\cdot\text{m}^{-1}$; (b) the data regressed reversible and irreversible width at half-height, w_{rev} and w_{irr} , and applied field at peak susceptibility, H_p .

Table 1. Standard error between the LangArc model parameters fitted against Magn97-PUC minor loop data at $12.7 \text{ kA}\cdot\text{m}^{-1}$ and $18.2 \text{ kA}\cdot\text{m}^{-1}$, and the measured experimental data at $12.7, 14.4, 16.5$ and $18.2 \text{ kA}\cdot\text{m}^{-1}$.

Parameter	Minor loop coercivity	Minor loop remanence	Maximum magnetisation	Hysteresis loop power	Predicted temperature
Standard error	$40 \text{ A}\cdot\text{m}^{-1}$	$58 \text{ A}\cdot\text{m}^{-1}$	$437 \text{ A}\cdot\text{m}^{-1}$	$2.3 \text{ W}\cdot\text{m}^{-3}\cdot\text{Hz}^{-1}$	$9.4 \text{ }^\circ\text{C}$

value was used, to ensure an equal weighting between each parameter in the least squares method. Defining each parameter (minor loop coercivity, remanence, maximum magnetisation and power) as k_i :

$$k_i = f(T, \hat{H})_i \quad (27)$$

$$\text{Error} = \sum \left(\frac{k_i^{\text{predicted}}}{k_i^{\text{measured}}} - 1 \right)^2 \quad (28)$$

The dataset for the minor hysteresis loops collected for sample Magn97-PUC were collected using a pulse heating method, in which the field was turned on and the instantaneous magnetic field measured. The field was then turned off and allowed to cool back to the target temperature to remove any rise in temperature due to induction heating of the sample. The sample and measured temperature converge in a pulse heating method when the rise in temperature is small [16]. The predicted and measured temperature for this data is given in figure 6. This data were not used to tune the LangArc model, and there is a good correlation between the measured and model predicted temperatures.

Figure 6 demonstrates that the LangArc model can be used to successfully infer the temperature of a magnetic sample based on a pulse heating method, which has been used to ensure that the sample and the thermocouple are at the same temperature. Magnetic induction is a very effective method of

heating. Under a continuous applied field it can give rise to very rapid heating of the sample, whereas the thermocouple will be subject to thermal lag [3], leading to a difference in the temperature between the sample and the thermocouple. Figure 7 shows the measured and LangArc inferred temperature under the continuous heating of sample Magn97-PUC at $18.2 \text{ kA}\cdot\text{m}^{-1}$ and approximately 260 kHz, based on unpublished data from Noble *et al* [6].

The difference between the temperature inferred from the pulse-heating validated LangArc model and the type-E thermocouple peaks at approximately $180 \text{ }^\circ\text{C}$. The ability to accurately measure the temperature during rapid heating justifies the development of this new tool. It will be of particular use in preventing a significant overshoot past the target reaction temperature during the rapid start-up of induction heated reactors, where excess reactor temperatures can lead to unwanted side reactions, loss of selectivity, thermal degradation of products and coking reactions that foul the this is reaction sites.

4. Discussion

Figure 6 indicates that a multi-variable regression against hysteresis loop parameters, using a model such as the Langevin-arctangent model, is reasonably accurate in determining the sample temperature, with a standard error of $9.4 \text{ }^\circ\text{C}$. The application of the LangArc model overcomes the issues around multiple values of temperature for a give value of power and

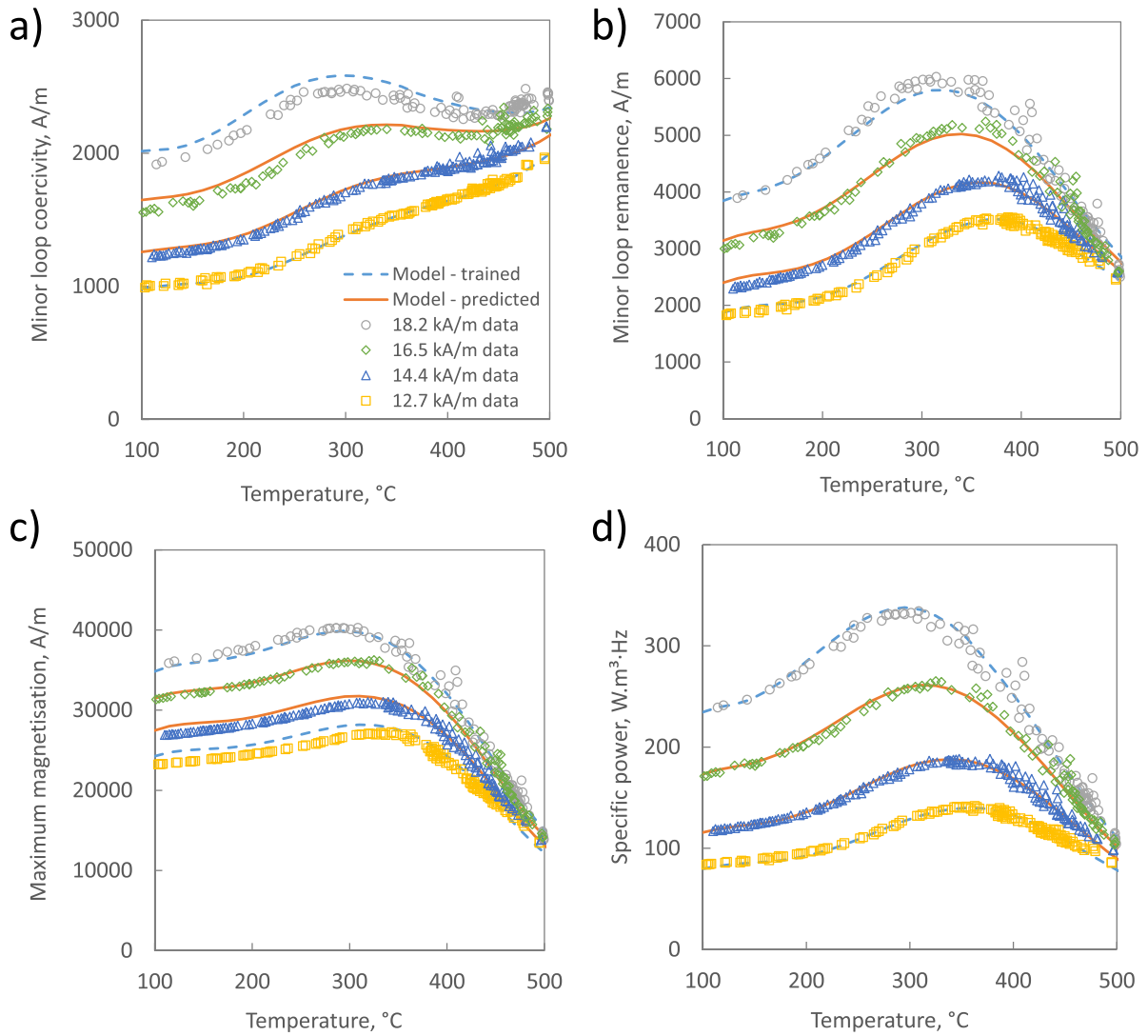


Figure 5. LangArc model tuning data set at $12.7 \text{ kA}\cdot\text{m}^{-1}$ and $18.2 \text{ kA}\cdot\text{m}^{-1}$ (dashed lines), and model predicted data at $14.4 \text{ kA}\cdot\text{m}^{-1}$ and $16.5 \text{ kA}\cdot\text{m}^{-1}$ (solid lines) for minor hysteresis loops of sample Magn97-PUC. A good fit is shown when the model is compared to the measured data (points) for: (a) minor loop coercivity (r^2 : 0.977); (b) minor loop remanence (r^2 : 0.979); (c) maximum magnetisation (r^2 : 0.986); and (d) hysteresis loop power (r^2 : 0.988).

improves the temperature resolution around the peak values of hysteresis loop parameters. This approach is successful in the magnetite example provided. We note that the minor loop remanence and power both have flat peaks in the same temperature region (figure 5). These hysteresis loop parameters are solely related to the irreversible magnetisation terms: the irreversible fraction contribution to saturation magnetisation $M_s(I-\varepsilon_r)$, the irreversible width at half height of the susceptibility function, w_{irr} , and the major loop applied field at peak coercivity, H_p . The implication is that the maximum magnetisation and minor loop coercivity terms are essential in improving the accuracy of the temperature prediction around the peak values in remanence and power. The maximum magnetisation and minor loop coercivity contain additional terms related to the reversible magnetisation function, implying that the reversible magnetisation effects need to be adequately represented as part of a temperature inference model. The developments made in transforming the LineArc model to the

LangArc model allow for improvements to the reversible magnetisation function that are based in magnetic theory rather than simply empirical.

The saturation magnetisation at zero Kelvin, M_{s0} , predicted by the model fit to Magn97-PUC data is $287 \text{ kA}\cdot\text{m}^{-1}$, compared to a value of $485 \text{ kA}\cdot\text{m}^{-1}$ for bulk multi-domain magnetite [17]. Surface effects are known to play a role in the saturation magnetisation, as discontinuities in the regular crystal structure of a magnetic material at its surface can lead to a reduction in the number of electrons that contribute to the particle's dipole moment. As particle sizes get smaller, the relative surface area per unit volume increases, enhancing this effect for small particle sizes. This reduction in saturation magnetisation has been reported to occur below 200 nm in magnetite [18], and hence is likely to be of relevance to Magn-97-PUC, which has a mean particle size of 97 nm. The sample also appears to have a large reversible fraction, especially as the temperature increases towards the Curie point.

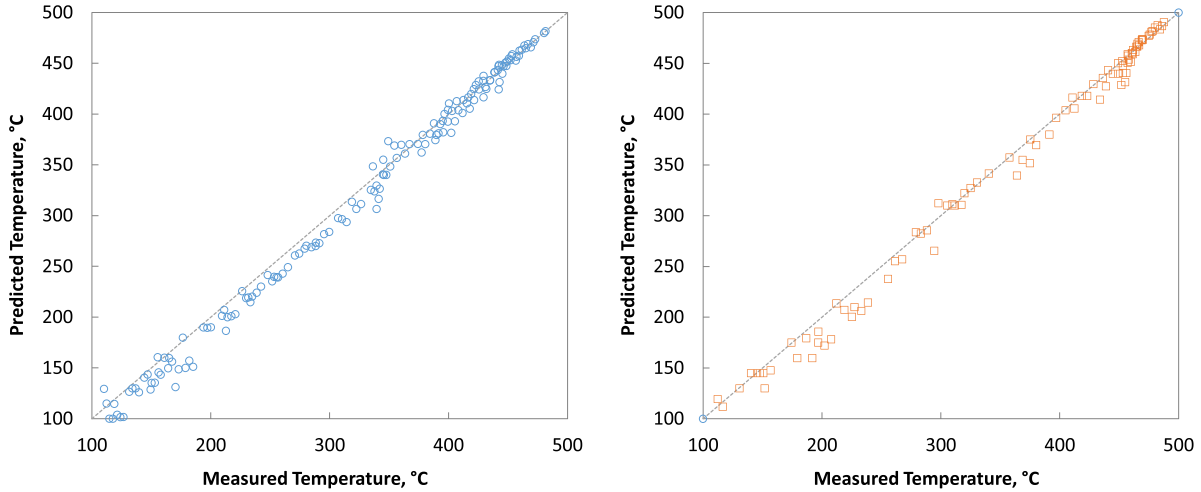


Figure 6. The measured temperature and predicted temperature using the LangArc model parameters fitted in figure 4 for pulse heating of magnetite powder sample Magn97-PUC at applied field strengths of $14.4 \text{ kA}\cdot\text{m}^{-1}$ (left) and $16.5 \text{ kA}\cdot\text{m}^{-1}$ (right). The standard error in the predicted temperature is $9.4 \text{ }^\circ\text{C}$; both fits have an r^2 value of 0.994.

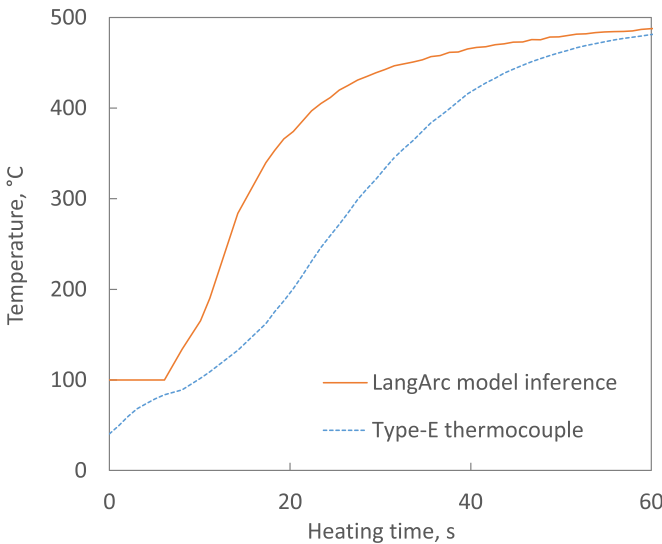


Figure 7. The continuous heating curve for magnetite sample Magn97-PUC induction heated from room temperature at $18.2 \text{ kA}\cdot\text{m}^{-1}$ and approximately 260 kHz, showing the measured reading on the type-E thermocouple and the inferred temperature from the tuned LangArc model. The thermocouple is subject to lag, whereas the magnetic field measurements are directly related to the temperature of the magnetic material. The LangArc minimum temperature is $100 \text{ }^\circ\text{C}$ due to the limit in the steady state data used to fit the model. The difference between the measured temperature and inferred temperature peaks at $180 \text{ }^\circ\text{C}$.

The model has been tuned and tested at a frequency of approximately 260 kHz and may need further fitting to infer temperature at different frequencies due to the possibility of rate-based superparamagnetic resonance within the sample.

This paper develops a proof-of-concept in which a magnetic field measurement can be used to infer the average temperature of a cross section of a heated bed or could be used

to build a small ‘magnetic field’-based temperature instrument for measuring a local temperature at a point within a bed. Localised measurement is of particular relevance to larger scale susceptor beds, as the voltage (EMF, ϵ) induced in a magnetic pick-up coil is proportional to the area of the coil in accordance with Lenz’ law (equation (29)). This can result in very large voltages for larger radius coils as follows:

$$\epsilon = -N\mu_0 a \frac{dH}{dt} \quad (29)$$

$$H = \hat{H} \cdot \sin(2\pi ft) \quad (30)$$

$$\hat{\epsilon} = 2\pi f N \mu_0 \hat{H} a. \quad (31)$$

For a single turn pick-up coil placed in a sinusoidal field with peak applied field strength, \hat{H} , of 10 kA m^{-1} and frequency, f , of 25 kHz, a coil with a 1 cm radius experiences a peak induced voltage of 0.6 V, whereas a 50 cm radius coil experiences an induced voltage of 1550 V. High voltages can be problematic for a number of reasons. They require wires with greater electrical insulation around the outside to prevent electric shocks and sparks, which could cause an ignition hazard when used in a chemical process with flammable material present. It is therefore likely that there is a practical upper limit to the size of a pick-up coil used for magnetometry in an induction heated bed.

The authors acknowledge that the data presented in this paper are limited to a single magnetic material, magnetite. An arctangent-only model has previously been used to approximate the major hysteresis loops of magnetite, hematite and goethite [19, 20], and the LineArc model has been shown to approximate hysteresis loops for magnetite and maghemite [6]. These materials cover both ferro- and ferri-magnetic

materials with inverse spinel, orthorhombic and rhombohedral crystal lattice structures, implying that the LangArc model could be widely applicable across a range of soft magnetic materials, particularly those with a significant paramagnetic fraction. This paper also presents an approach for modelling families of hysteresis loops using a number of different sigmoidal functions. It is proposed that a linear superposition of a number of sigmoidal curves should provide sufficient flexibility for this approach to be generalised to a wide range of hysteretic magnetic materials.

5. Conclusions

This paper outlines the key features that are required from a magnetic hysteresis model that is practically applicable in induction heated chemical reactors. The LineArc model has previously been successfully applied to the minor hysteresis loops of magnetite and maghemite but cannot sufficiently replicate the major hysteresis loop due to the presence of a linear term. It has been developed into the LangArc model by replacing the linear term with a Langevin function to represent a paramagnetic fraction within the sample. The LangArc model fits the major hysteresis loop data of magnetite powder dispersed in epoxy cement from 150 °C to 550 °C. The LangArc model supersedes the LineArc model and is shown to reduce to the LineArc model at low applied field strengths. In addition, it has been shown that the LangArc parameters are related to the major loop properties, such as coercivity and remanence.

The LangArc model has been fitted to minor loop data for bulk magnetite powder across an applied field strength range of 12.7–18.2 kA·m⁻¹ and is able to accurately reproduce the shape parameters of these hysteresis loops with a minimum r^2 value of 0.977. The LangArc parameters are over-specified in the Rayleigh region and a theoretical basis is provided to explain this phenomenon. In the pulse heating experiments, which are used to ensure that the thermocouple and sample are at the same temperature, the fitted LangArc model can be used to infer the temperature of the magnetite sample and compares favourably to the measured temperature with an r^2 value of 0.994 and standard error of 9.4 °C. The use of a multi-parameter hysteresis loop fit therefore allows for the magnetic measurements to be resolved into a single, unique temperature point. The LangArc model provides better modelling of the reversible magnetisation term than the LineArc model, improving the prediction of the minor loop coercivity and maximum magnetisation and providing better temperature resolution around the peak power conditions. Applying the LangArc method to a continuous heating profile shows that the sample temperature may be 180 °C hotter than measured due to thermocouple thermal lag. The magnetically inferred temperature technique is therefore a useful addition to the toolkit of induction heating instrumentation as it allows for accurate temperature measurements during rapid transient heating.

In an ideal model, data would be fitted to major hysteresis loops at the desired operating frequency to determine the

LangArc model parameters. These would be used to reproduce the minor hysteresis loop shape and properties. Due to the differences between the VSM sample (dispersed in epoxy cement) and the *in-situ* magnetometry (loose powder), a direct comparison is not possible. Further investigation across a wider range of magnetic materials and field strengths will allow insight into whether the LangArc model is intrinsically related to the underlying magnetisation mechanisms or is simply a convenient fit to the minor loop data. Regardless, the work in this paper demonstrates that it is an important step forwards in measuring power and temperature in induction-heated chemical reactors.

Data availability statement

The data that support the findings of this study are openly available at the following URL/DOI: <https://doi.org/10.15125/BATH-01316>.

Acknowledgments

The authors gratefully acknowledge the Material and Chemical Characterisation Facility (MC²) at the University of Bath (<https://doi.org/10.15125/mx6j-3r54>) for technical support & assistance in the materials characterisation.

This work was supported by the Engineering and Physical Sciences Research Council grant EP/L016354/1.

ORCID iDs

Jonathan P P Noble  <https://orcid.org/0009-0005-7284-2797>

Simon J Bending  <https://orcid.org/0000-0002-4474-2554>

Alfred K Hill  <https://orcid.org/0000-0003-4324-3822>

References

- [1] Ceylan S, Coutable L, Wegner J and Kirschning A 2011 *Chem. Eur. J.* **17** 1884
- [2] Wang W, Tuci G, Duong-Viet C, Liu Y, Rossin A, Luconi L, Nhut J-M, Nguyen-Dinh L, Pham-Huu C and Giambastiani G 2019 *ACS Catal.* **9** 7921
- [3] BS EN 61515 2016 BSI Standards: mineral insulated metal-sheathed thermocouple cables and thermocouples
- [4] Jiles D 2015 *Introduction to Magnetism and Magnetic Materials* (Chapman and Hall) (<https://doi.org/10.1201/b18948>)
- [5] Bertotti G 1998 *Hysteresis in Magnetism: For Physicists, Materials Scientists, and Engineers* (Academic)
- [6] Noble J P P, Bending S J, Sartbaeva A, Muxworthy A R and Hill A K 2021 *Adv. Energy Mater.* **12** 2102515
- [7] Fiorillo F, Appino C and Pasquale M 2006 *Sci. Hysteresis* **3** 1
- [8] Ponomarev Y F 2007 *Phys. Met. Metallogr.* **104** 469
- [9] Takács J 2018 *Appl. Math. Nonlinear Sci.* **3** 403
- [10] Nowicki M, Szewczyk R and Nowak P 2019 *Materials* **12** 1549
- [11] Mohan Kant K, Sethupathi K and Ramachandra Rao M S 2008 *J. Appl. Phys.* **103** 1

- [12] Raghunathan A, Melikhov Y, Snyder J E and Jiles D C 2009 *IEEE Trans. Magn.* **45** 3954
- [13] Dunlop D J and Özdemir O 2010 *Rock Magnetism: Fundamentals and Frontiers* (Cambridge University Press) (<https://doi.org/10.1017/CBO9780511612794>)
- [14] Yoon S 2011 *J. Korean Phys. Soc.* **59** 3069
- [15] Hadjipanayis G C 1997 *Magnetic Hysteresis in Novel Magnetic Materials* (Springer) (<https://doi.org/10.1007/978-94-011-5478-9>)
- [16] Périgo E A, Hemery G, Sandre O, Ortega D, Garaio E, Plazaola F and Teran F J 2015 *Appl. Phys. Rev.* **2** 041302
- [17] Li Q, Kartikowati C W, Horie S, Ogi T, Iwaki T and Okuyama K 2017 *Sci. Rep.* **7** 1
- [18] Mascolo M C, Pei Y and Ring T A 2013 *Materials* **6** 5549
- [19] Vasquez C A and Fazzito S Y 2020 *Stud. Geophys. Geod.* **64** 114
- [20] Milovanovic A M and Koprivica B M 2015 *Electromagnetics* **35** 155